RSC Advances

ROYAL SOCIETY OF CHEMISTRY

www.rsc.org/advances

Synthesis and highly efficient supercapacitor behavior of novel poly pyrrole / ceramic oxide nanocomposite film

A. Ehsani[a*], H. Mohammad Shiri[b], J. Shabani-Shayeh[a]

[a]*Department of Chemistry, Faculty of science, University of Qom, P. O. Box 37185-359, Qom, Iran.*

[b]*Department of Chemistry, Payame Noor University, Iran*

*****Corresponding author:

E-mail address: ehsani46847@yahoo.com and a.ehsani@qom.ac.ir

Abstract

A novel method of electrochemical synthesis of yttrium aluminum garnet (YAG: $Al_5Y_3O_{12}$) is successfully developed in the mixture of $YCl3_3$ and $AlCl_3$ aqueous solution. The electrosynthesized YAG are further annealed and characterized by X-ray diffraction (XRD) and scanning electron microscopy (SEM). Ppy/YAG thin film electrode is synthesized electrochemically for electrochemical supercapacitor. Scanning electron micrographs clearly reveals the formation of nanocomposites on the surface of working electrode. Different electrochemical methods including galvanostatic charge–discharge (CD) experiments, cyclic voltammetry (CV) and electrochemical impedance spectroscopy (EIS) are carried out in order to investigate the applicability of the system as a supercapacitor. Based on the electrochemical results obtained, Ppy/YAG gave higher specific capacitance, power and energy values than Ppy at a current density of $1mAcm^{-2}$. Specific capacitance (SC) of Ppy and Ppy/YAG electrodes are calculated using CV method are 109 and 254 Fg^{-1}, respectively. This work introduces new nanocomposite materials for electrochemical redox capacitors with advantages including long life cycle and stability in an aqueous electrolyte to that of commonly used ruthenium based pervoskites.

Keywords: Supercapacitor, Ppy, YAG, Nanoparticles, Impedance.

Introduction

Electrochemical capacitors (ECs), known as supercapacitors, are charge-storage devices that capable of very fast charges and discharges, with a unique combination of high power, high energy and long lifetime [1, 2]. ECs with these unique properties can bridge the gap between batteries and capacitors, offering great potentials in applications such as starting automotives and regenerating of brake energy. To date, carbon [2–6], transition metal oxides [4, 5] and conducting polymers (CPs) [6] have been identified as most promising materials for ECs. Each material has its own unique advantages and disadvantages for supercapacitor applications.

Some of the most famous CPs includes polyaniline, polypyrrole, polythiophene and their derivatives. Polyaniline (PANI) and polypyrrole (Ppy) are the most promised CP for application as an electrode in redox supercapacitors [7]. Charge storage mechanism in CPs is followed by loss of electrons and formation of polycations, causing the anions in the solution to intercalate into the CP in order to maintain electroneutrality. Repeating charge-discharge process leads to accumulation of stress on polymer, which is related to poor cycle life [8]. One of the solutions for this problem is using nano materials to synthesize nanocomposites. In these nano composites, the nanoparticles are dispersed in monomer solution to make an entangled polymer matrix [9, 10].

A lot of attempts are going on to increase the capacitance values of the electrode with the minimum investment. As is highly expensive, alternative metal oxides are being explored. Most of the attempts are made with a small amount of ruthenium which served as an excellent metal oxide for supercapacitor, with other materials for better performance. One of the attempts to obtain the better performance of supercapacitor electrode was to use pervoskite like $SrRuO_3$ containing one of element ruthenium [11, 12]. It is expected that the combined metal oxides, a pervoskite i.e. $BiFeO_3$ has to show the similar or perhaps better performance. The bismuth iron

oxide in five crystallite phases i.e. $BiFeO_3$, Bi_2 Fe_4O_9 and Bi3 Fe_5O_{12} is well known. That means this material may sustain the charges in its phases during the electrochemical changes [12].

YAG has revealed many potential properties, for optical and structural applications. Conventionally, YAG was prepared by the solid–state combustion techniques. However, two intermediate phases yttrium aluminum perovskite (YAP) and yttrium aluminum monoclinic (YAM) are produced during the heating period using this method. The hydrothermal method [13, 14] in this case, with higher pressure over 40 MPa was required to form YAG. The sol-gel method [15], although the sol-gel seems to be a potential method, the precursory solution was so complicated that a high temperature (1050°C) annealing process is essential for removing the impurity residues[16] Since the luminescent materials for flat panel displays have attracted more attention, the research activities aimed at developing these types of materials in the form of films are increasingly required [17]. Therefore, developing a simple process by using low cost equipment, at lower temperature and at ambient atmosphere, will become more attractive for commercialization. In this report, YAG thin film was prepared by pulse electrochemical synthesis in the mixture of YCl_3 and $AlCl_3$ aqueous solution.

There are two methods for preparation of conductive polymer/nanocomposites: chemical method in which an oxidizing agent is used and in situ polymerization occurs [18, 19]. Another method is electrochemical synthesis of conductive polymeric nano composites in which nano materials are dispersed in a monomer solution and nanocomposite are formed by electropolymerization [20-26]. Electrodeposition is a powerful and interesting process that can be applied in numerous fields. Films can be synthesized at a low or room temperature because of high energy density accumulated in solution near the electrode surface. The advantages of electrodeposition compared with other techniques include low cost for raw materials and

equipments, capability of controlling composition and morphology by varying electrochemical parameters and the ability to deposit films on a complex surface. This is probably the easiest, non-vacuum and suitable method to prepare electrodes of large area. In the present work, room temperature electrochemically synthesized Ppy/YAG electrode is presented as an efficient potential candidate in supercapacitor application. Our goals in this paper were increasing the capacitance of Ppy electrode by using YAG nanoparticles to form a composite electrode and moreover increase the cycle ability of the electrode.

2. Experimental

2.1. Reagent and materials

All the chemical materials used in this work, obtained from Merck Chemical Co., were of analytical grade and used without further purification. Double distilled water was used throughout the experiments. Pyrrole (py) was doubly distilled and the resulting colorless liquid was kept in the dark at 5°C.

2.2. Apparatus

All electrochemical experiments were carried out by an Autolab General Purpose System PGSTAT 30 (Eco-chime, Netherlands). A conventional three electrode cell with an Ag/AgCl reference electrode (Argental, 3 M KCl) was used in order to carry out the electropolymerization of the Ppy. A platinum wire with a diameter of 0.5 mm and an exposed area of 0.65 cm^2 was used as the counter electrode. A glassy carbon electrode with an area of 0.03 cm^2 was used as the working electrode. A wide frequency range of 10 mHz to 100 kHz was used in EIS. Morphological investigations of the polymeric films were carried out by using SEM (Philips XL 30). X-ray diffraction patterns were obtained from an X-ray diffrac-tometer (PANalytical X'Pert-Pro) with a Cu-K^{α} monochromatized radiation source and an Ni filter.

2.3. Preparation of YAG nanoparticles via cathodic pulse electrochemical deposition

YAG has been electrosynthesized in conventional three electrode cell with 316L stainless steel (100× 50× 0.5 mm) as a working electrode centered between two parallel graphite (100× 50× 5 mm) as a counter electrodes and saturated calomel electrode (SCE) as a reference electrode. Electrolyte were 0.005M YCl_3. $6H_2O$, 0.008 M $AlCl_3.6H_2O$ (with

respect to YAG stoichiometry) dissolved in double-distilled water. The pH of the chemical bath was adjusted to 2.7 by adding concentrated HCl solution. YAG thin films were deposited on the surface of the stainless steel by using the pulse voltage mode, with applying a peak current density of 5mA.cm^{-2} and t_{on}=t_{off}=1ms for 20 min in the 60°C. The square wave potential (-0.7 V respect to SCE) was applied in the cathodic electrodeposition of YAG. After electrodeposition process, steel electrodes were washed, dried at room temperature for 36 h and deposited powders were scrapped from the steel electrodes for further process. Heat-treatment of the hydroxide powders was conducted at the 1200°C in dry air atmosphere for 2 h *via* electrical furnace with heating rate of 5°C.min^{-1}. Transparent powders of YAG finally formed after being annealed at 1200°C. YAG powder was characterized by means of X-ray diffraction as shown in Fig. 1. In this figure, a strong and sharp peak at 2θ = 18.19, 29.74 and 33.42^{0} are characteristic of YAG.

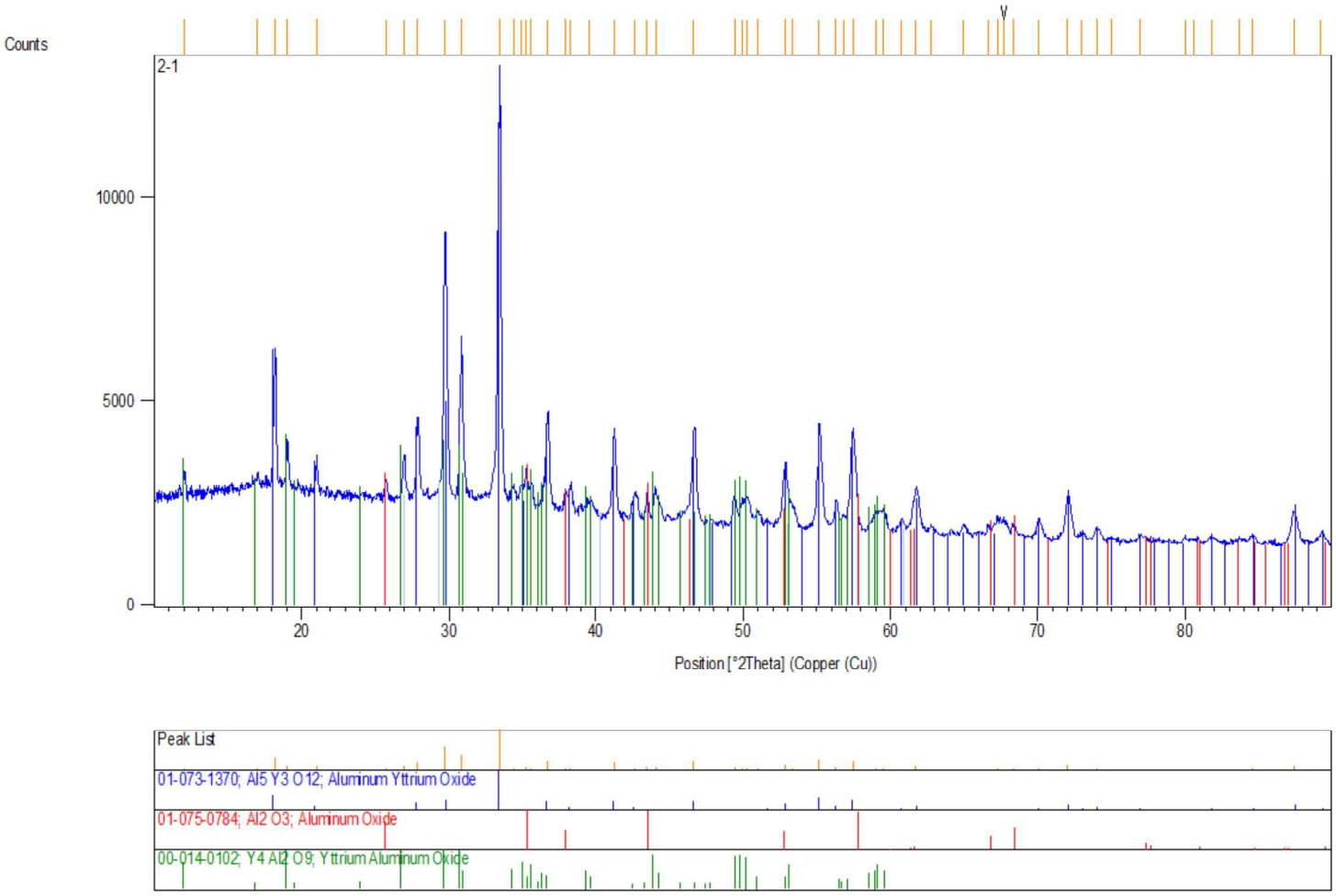

Fig. 1. XRD spectrum of YAG

SEM and EDX have been applied for analysis of the compound. EDS spectrum and SEM image of YAG ($Al_5Y_3O_{12}$) have been shown in figure 2 and figure 3 respectively. As evident from SEM image and EDS spectrum, formation of YAG nanoparticles have been confirmed.

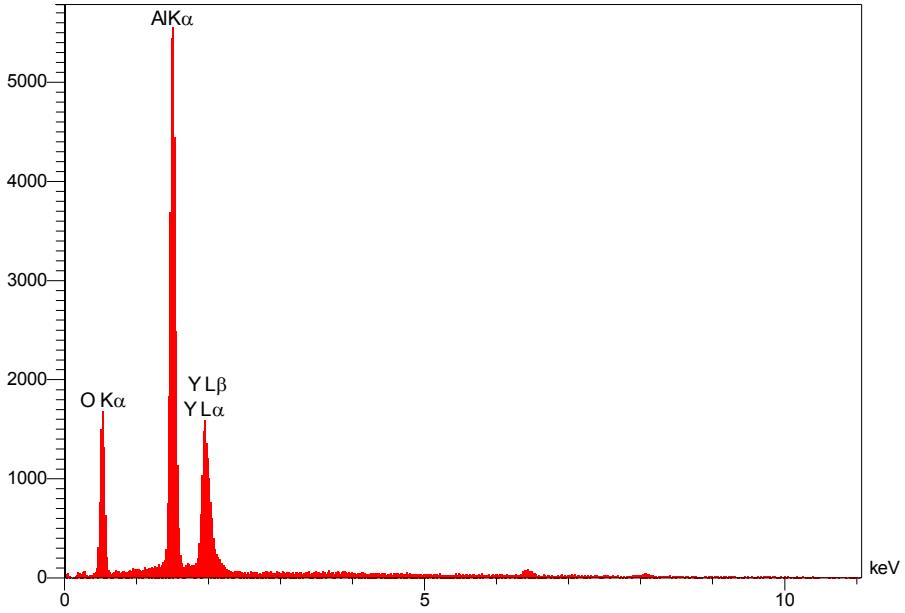

Fig. 2. EDS spectrum of electrosynthesized YAG ($Al_5Y_3O_{12}$)

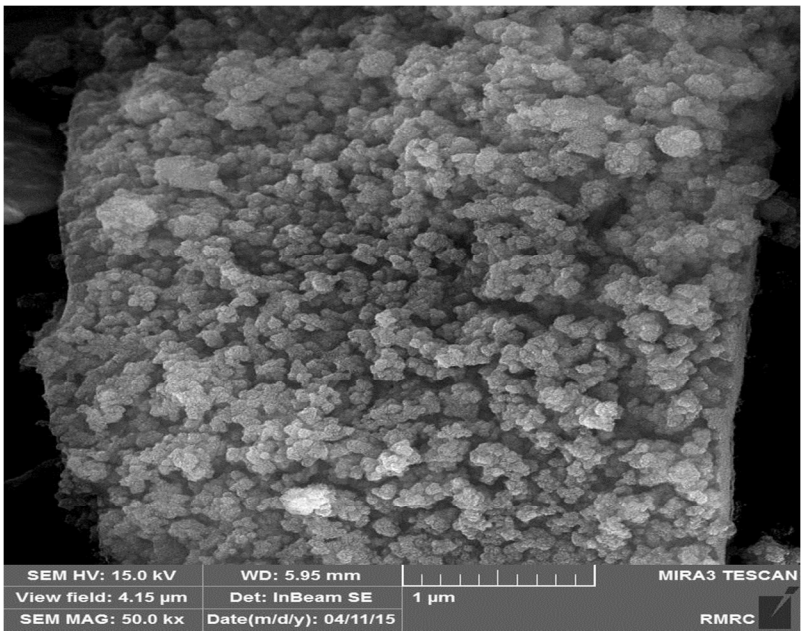

Fig. 3. SEM image of YAG ($Al_5Y_3O_{12}$)

2.4. Synthesis of Ppy and Ppy/YAG nanocomposite

Ppy/YAG nanocomposite was synthesized electrochemically by cyclic voltammetry in 0.1M KCl solution contained Py monomer (0.1M), YAG (0.5% wt) and sodium dodecyl sulfate (0.005 M) that dispersed in solution by sonication. Ppy electrode was synthesized in same solution without YAG. Electropolymerizations were conducted by 10 consecutive cycles at the sweep rate of 50 $mV.s^{-1}$ in the potentials between 0.0 to 1 V. The mass of Ppy films was approximated assuming a current efficiency for the electropolymerization process of 100%, using Faraday's law. SEM images of Ppy/YAG film are shown in Fig. 4.

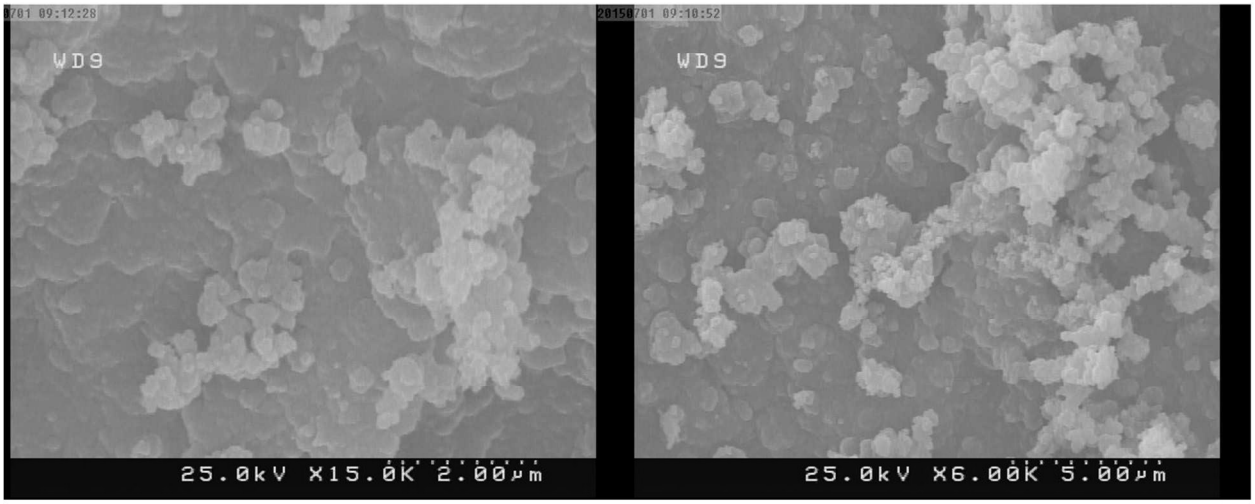

Fig. 4. SEM images of Ppy/YAG nanocomposite in different magnification and quantitative results of EDS analysis.

3. Results and discussion

Figure 5 shows the CVs of Ppy and Ppy/YAG electrodes in 0.1 M H_2SO_4 solution at the sweep rate of 25 $mV.s^{-1}$. As observed, the capacitance of composite electrode is about two times greater than that of Ppy electrode, which shows using YAG in Ppy electrode enhances the capacity of the electrode. The synergetic effect resulting from the interactions of Ppy and YAG nanoparticles may affect the shape of CV curves. The CV of Ppy/YAG electrode exhibits nearly symmetrical rectangular shapes in potential window, that shows the incorporation of YAG in Ppy matrix not only increase the capacitance of composite due to redox transitions of YAG between different valence states, but also save it's ideal capacitive behavior. Due to electrostatic interactions, ions in the solution migrate to the electrode to counterbalance the charge on the electrode i.e. the protons travel from one electrode to the other through the electrolyte during charge and discharge. The movement of electrons occurs at the same time through the current source or the external load. Thus, the current–voltage profile of the composite electrode is symmetric.

Specific capacitance (SC) of electrodes is calculated from CV curves using the following equation [27]:

$$C = \frac{I}{mv} \qquad (1)$$

where I is the current, m is the mass of reactive material and ν is the potential scan rate.

The SC of Ppy and Ppy/YAG electrodes were found to be 109 and 254 $F.g^{-1}$, respectively. While Park et al. [28] have obtained the specific capacitance for lead ruthenate pyrochlore up to 160 $F.g^{-1}$. Similarly, for lead ruthenate pyrochlore, Cao et al. [29] and Bang et al. [30] have obtained the specific capacitance of 90 and 100 $F.g^{-1}$. These values are certainly better than those obtained

from a pervoskite SrRuO3, co-precipitated at 800 C (specific capacitance = 8 $F.g^{-1}$) by Mehrens et al. [31].

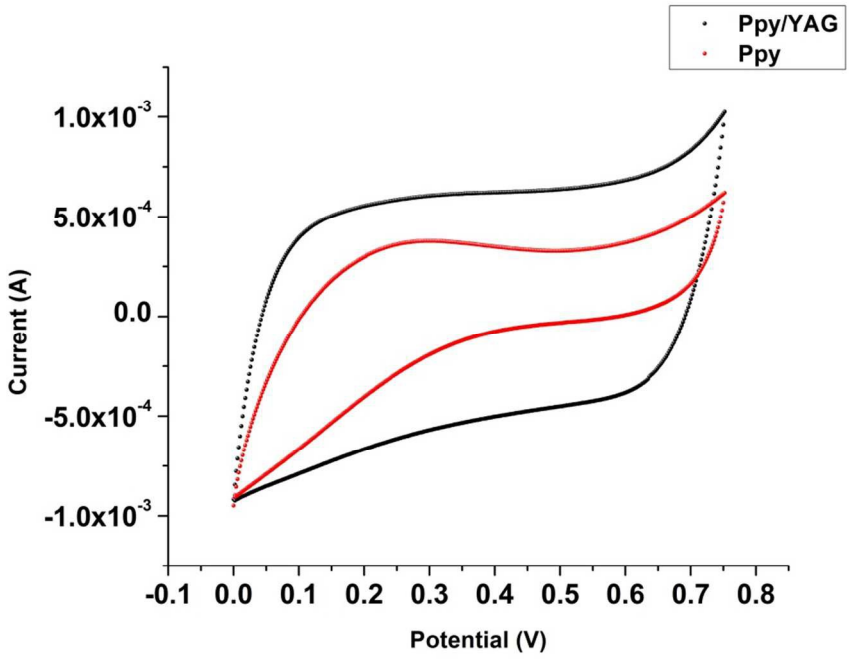

Fig. 5. Cyclic voltammograms of Ppy and Ppy/YAG electrodes in 0.1M H_2SO_4 at the sweep rate of 25 $mV.s^{-1}$.

Figure 6 shows CV curves of Ppy/YAG electrode at various scan rates in 0.1 M H_2SO_4 solution. As it can be seen, the excellent capacitive performance of the Ppy/YAG electrode is also verified from these curves. According to CV results, by increasing scan rate, the current response of the composite film increases. This behavior can be related to an ideal capacitive of Ppy/YAG electrode. Furthermore, the good rectangular CV shape of the Ppy/YAG electrode remains constant at the scan rate of $100mV.s^{-1}$. The deviation from rectangularity of CVs becomes obvious as scan rate increases. This phenomenon can be attributed to the electrolyte and film resistance, and this distortion is dependant on scan rate. By increasing the sweep rate, active sites will not have enough time for reaction on the surface of the electrode.

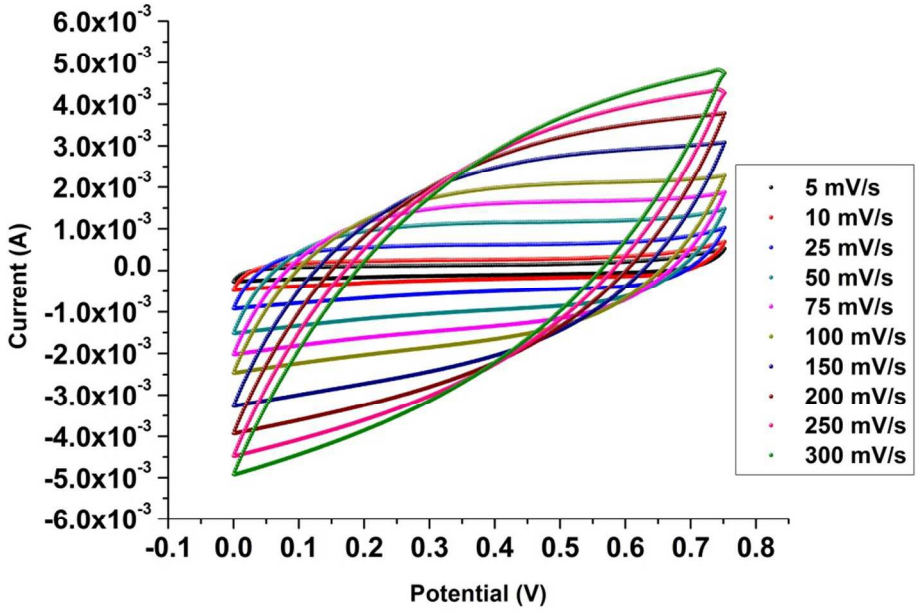

Fig. 6. CVs of Ppy/YAG electrode at different scan rates in 0.1 M H_2SO_4 in the potential window of -0.2 – 0.8 V.

Figure 7 shows the calculated specific capacitance of Ppy/YAG electrode as a function of scan rate. As observed, the capacitance of two electrodes decays over the entire range of scan rate, because in fast sweep rates just outer porosity are use and deeper those are not accessible for doping / undoing process. As can be seen in high scan rates the composite electrode losses it's SC with a reduction pattern same as Ppy electrode that shows Ppy/YAG doesn't block the porosities of polymer network. If these phenomena occurred, the reduction of SC in composite electrode was more than Ppy electrode.

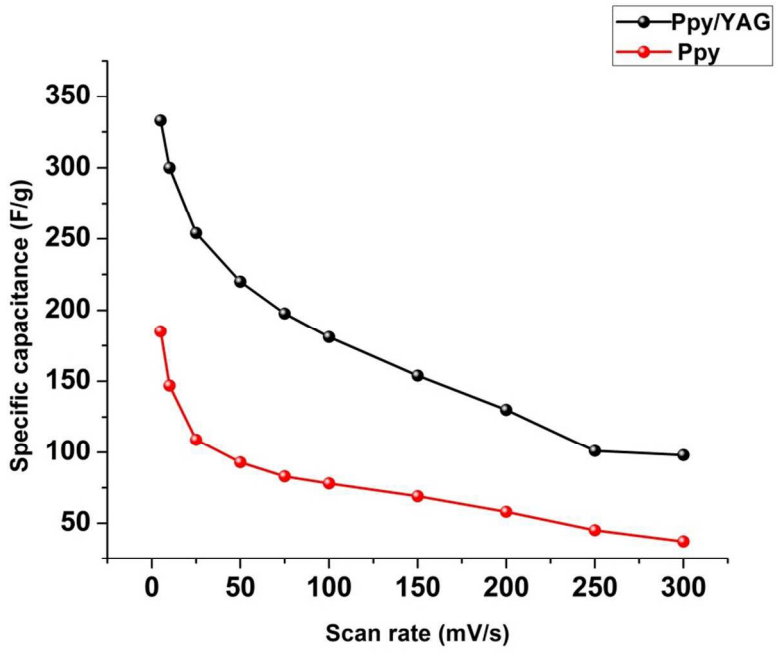

Fig. 7. Variations of the specific capacitance for Ppy and Ppy/YAG electrode as a function of the scan rate in 0.1M H_2SO_4 solution.

Galvanostatic charge/discharge method has been used to highlight the capacitance characteristic of Ppy/YAG composite electrode. Figure 8 shows the charge/discharge behavior of Ppy and Ppy/YAG electrodes in the potential range from -0.2 to 0.8 V at the current density of 2.0 $A.g^{-1}$. As it can be seen, a triangular shape between this potential ranges is observed that indicating good columbic efficiency and ideal capacitive behavior of Ppy/YAG as electrode for application in supercapacitors.

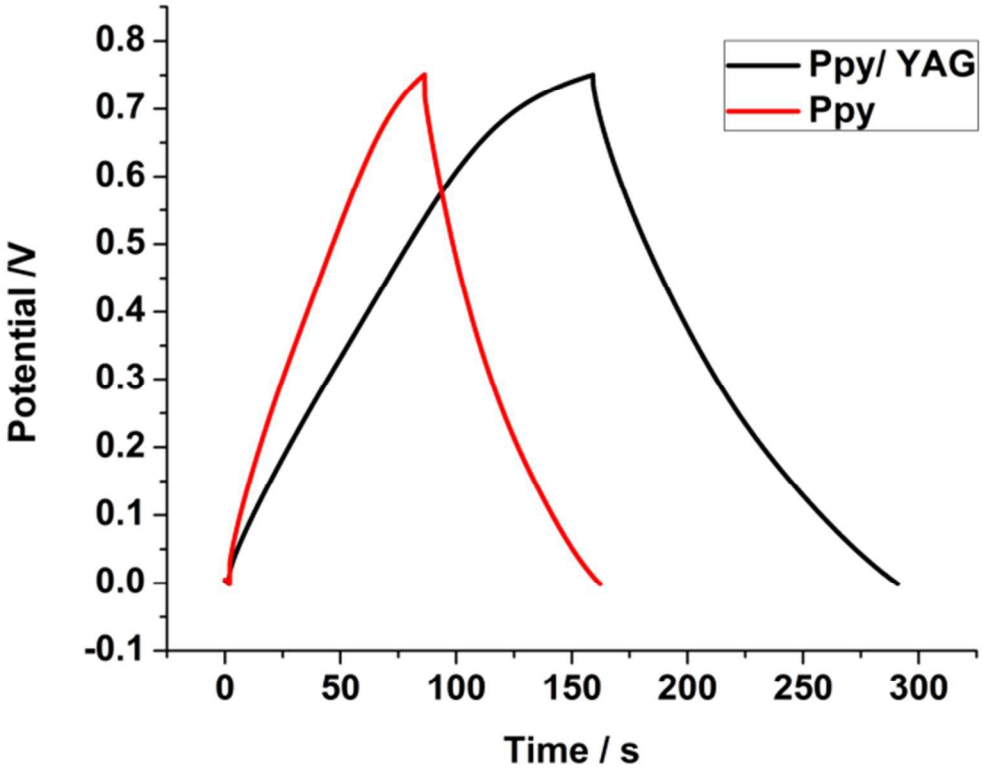

Fig. 8. Galvanostatic charge and discharge measurements of Ppy and Ppy/YAG electrode in 0.1M H_2SO_4 solution at the current density of 2.0 $A.g^{-1}$.

Figure 9 presents the charge−discharge curves of Ppy/YAG electrode at various specific currents of 2.2-16 $A.g^{-1}$. As it can be seen, by enhancing the specific current, specific capacitance values decrease due to intercalation of ions at the surface of the active materials in the electrode/electrolyte interface. On the other hand, when low specific current is used, the specific capacitance increases because there is enough time for insertion and deinsertion of the ions at the surface and deeper porosities of the active materials in the electrode/electrolyte interface. These phenomena can conclude from this data that in low density currents the voltage range in charge−discharge curves decreased. Here, SC has been measured according to the charge/discharge curves, using Eq. (2).

$$SC = \frac{i}{\left(-\frac{\Delta E}{\Delta t}\right)m} \quad (2)$$

where i is the applied current, -ΔE/Δt is the slope of the discharge curve after the voltage drop at the beginning of each discharge (ESR) and m is the mass of composite electrodes. The most SC for composite electrode is obtained when the current density for charge/discharge process is 2.2 $A.g^{-1}$.

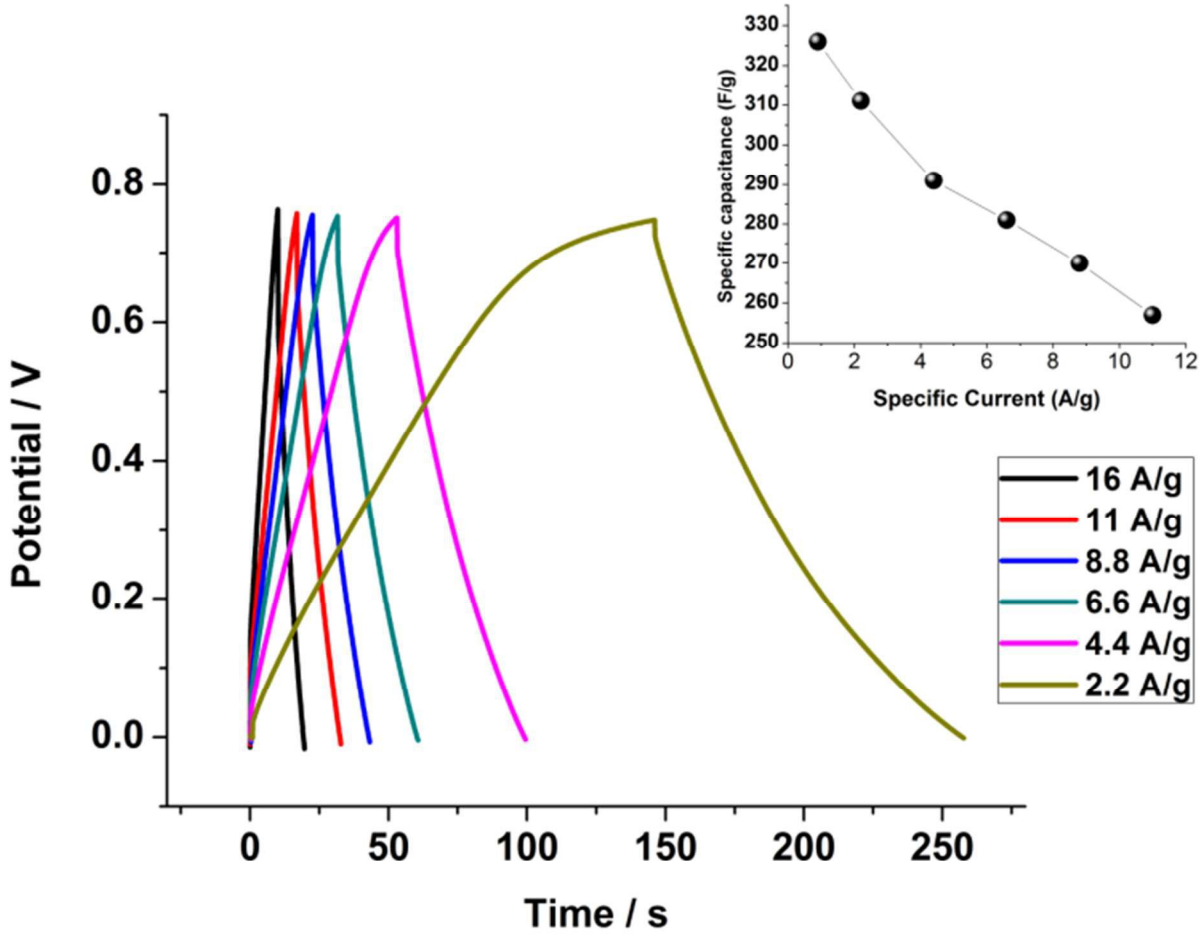

Fig. 9. Galvanostatic Charge-Discharge curves of Ppy/YAG electrode at 2.2-16 $A.g^{-1}$ in 0.1 M H_2SO_4 solution.

EIS method is performed to investigate the electrochemical supercapacitive and conductivity behaviors of the prepared Ppy/YAG electrode. Figure 10 shows Nyquist plots of Ppy and Ppy/YAG electrodes at open circuit potential. Intercept of the Nyquist plots is related to the equivalent series resistance arising from contributions of electronic and ionic resistances [32-35]. There is a semicircle in high frequencies which is related to the charge transfer resistance (R_{ct}) caused by the Faradic reactions and the double-layer capacitance (C_{dl}) at the contact interface between electrode and electrolyte solution. A resistance with the slope of the 45° in the curve that called Warburg resistance (Z_W) is a result of the frequency dependence of ion diffusion/transport in the electrolyte to the electrode surface. As observed, the magnitude of R_{ct} in Ppy/YAG electrode was smaller than that in Ppy electrode, which shows that the addition of YAG improves charge transfer performance of Ppy composite electrode. In the low frequency region, both electrodes exhibit a nearly linear branch, indicating a decreased diffusion resistance of the electrolyte ions in the electrode, as expected for a capacitor. The low frequency capacitance (C_{lf}) of each film was determined from the slope of a plot of the imaginary component of impedance at low frequency versus the inverse of frequency (f), using Eq. (3).

$$C_{lf} = \frac{1}{(2\pi f Z'')} \qquad (3)$$

It can be seen that Ppy/YAG electrode has more capacitance than Ppy electrode. The SC for Ppy and Ppy/YAG electrode were calculated 117 and 262 $F.g^{-1}$ respectively. These results also confirmed the data obtained by CV and charge-discharge methods.

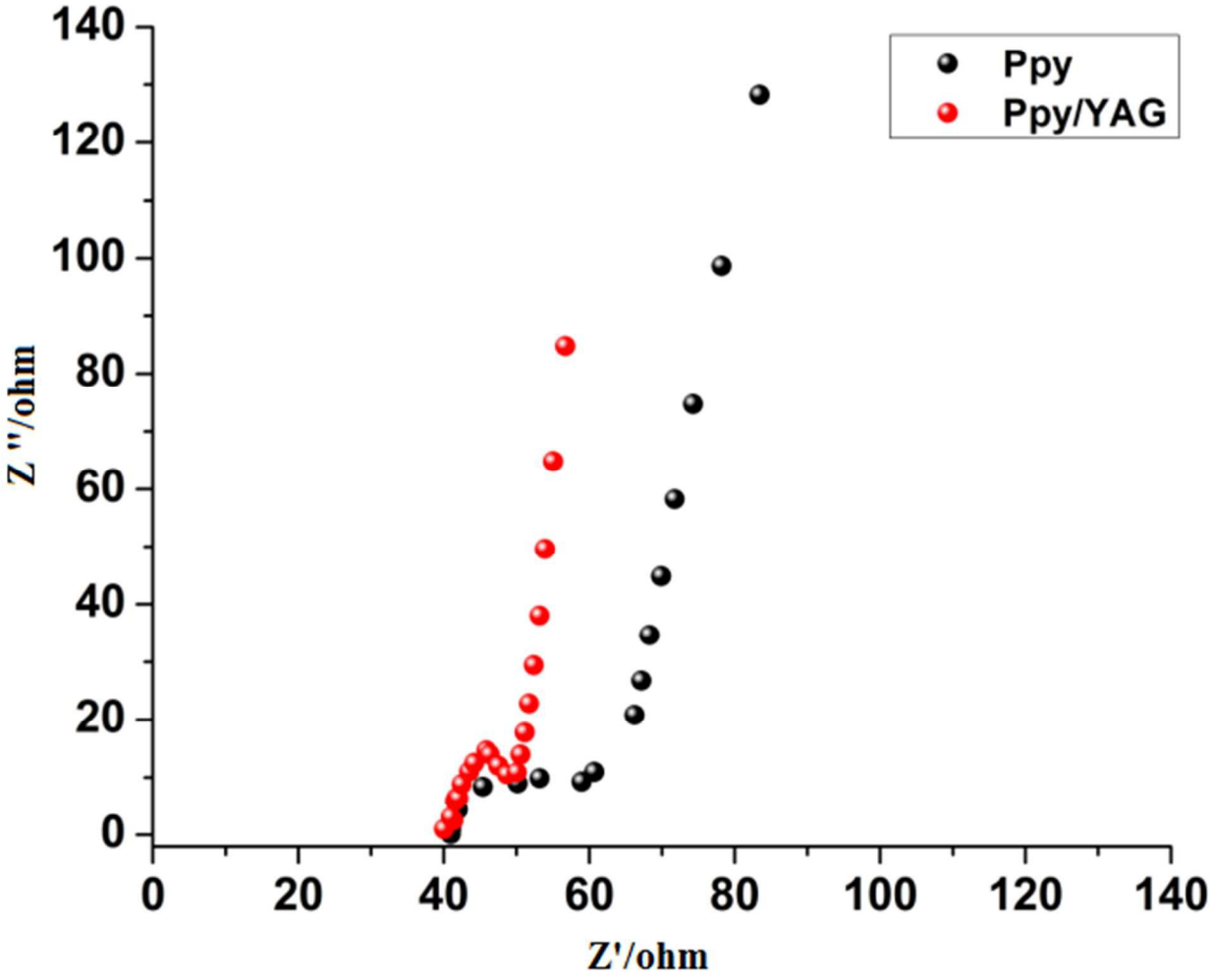

Fig. 10. Nyquist plots recorded from 10 kHz to 0.01 Hz with an ac amplitude of 5 mV for Ppy and Ppy/YAG electrode.

One of the most important parameters for practical application is cycling stability. As depicted in figure 11, stability of two electrodes is compared in terms of losing their capacities as stability percentage. The stability of electrode calculated from following equation:

$$\text{Stability} = \frac{C_n}{C_1} \times 100 \qquad (4)$$

In that C_n is the capacitance of electrode in each cycles and C_1 is capacitance of electrode in the first cycle. Using YAG in Ppy caused an excellent retention in stability percentage of Ppy/YAG

electrode suggesting the good stability toward long time charge-discharge applications. While the Ppy electrode loses its stability fast and gets 30% of capacitance of the first cycle after 20000s, Ppy/YAG electrode maintains its stability and saves more that 85% of its capacitance of the first cycle under consecutive cycles after 20000s.

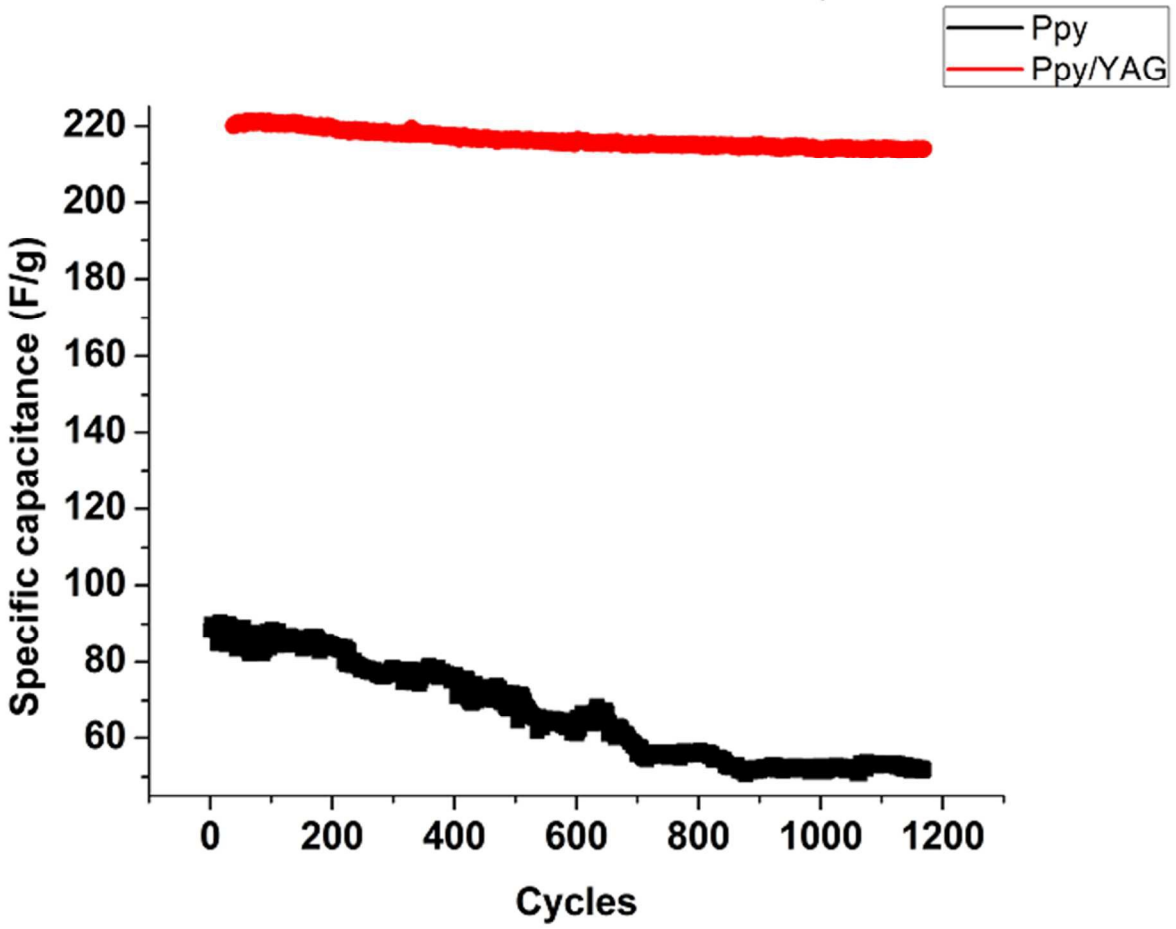

Fig. 11. stability of two electrode after consequtive cycles at 50mV.s^{-1} for 20000 s**.**

5. Conclusion

polyaniline and polypyrrole are usually used as an electrode in redox SCs. However, due to accumulation of stress on polymer during repeating charge-discharge process, the cycle life of pure CPs-based SCs is poor, which needs to be further improved. For this purpose, combining conventional CPs active material and nanomaterials to fabricate hybrid electrode has been considered to be one of the efficient avenues. In this paper, firstly YAG has been synthesized using pulse electrochemical deposition technology and then fabricated hybrid Ppy/YAG films by electro- polymerization of Ppy in the presence of YAG nanoparticles to serve as the active electrode for SCs. Compared with that of pure Ppy electrode (109 F g-1), the obtained hybrid Ppy/YAG film electrode exhibit much higher specific capacitance (254 F g-1) and excellent cycling stability. The enhanced capacitance performance may be attributed to the increase of conductivity and interfacial electron transfer dynamics by incorporation of ceramic oxide nanoparticles, as evidenced by electrochemical impedance spectral. Furthermore, Ppy/YAG composite electrode exhibited more highly stable capacitance retention during charge/discharge cycling and is therefore a promising candidate for long-term applications in high-performance supercapacitor.

Acknowledgements

The authors would like to express their deep gratitude to the Iranian Nano Council for supporting this work.

References

[1] B.E. Conway, Electrochemical supercapacitors, Kluwer Academic, Plenum Publishers, New York, 1999.

[2] J. Shabani Shayeh, P. Norouzi, M.R. Ganjali, *RSC Advances*, 2015, **5**, 20446-20452.

[3] R. Kotz, M. Carlen, *Electrochimica Acta*, 2000, **45**, 2483-2498.

[4] C. Zhang, H. Yin, M. Han, Z. Dai, H. Pang, Y. Zheng, Y. Lan, J. Bao, J. Zhu, *ACS Nano*, 2014, **8 (4)**, 3761–3770.

[5] A. Zolfaghari, H.R. Naderi, H.R. Mortaheb, *Journal of Electroanalytical Chemistry*, 2013, 697, 60-67.

[6] A. Ehsani, M. Mahjani, M. Jafarian, *Synthetic Metals*, 2012, **162** , 199-204.

[7] K.S. Ryu, K.M. Kim, N.-G. Park, Y.J. Park, S.H. Chang, *Journal of Power Sources*, 2002, **103**, 305-309.

[8] M.E. Roberts, D.R. Wheeler, B.B. McKenzie, B.C. Bunker, *Journal of Materials Chemistry*, 2009, **19** , 6977-6979.

[9] Y. Chen, M. Han, Y. Tang, J. Bao, S. Li, Y. Lan , Z. Dai, *Chem. Commun.*, 2015,**51**, 12377-12380.

[10] A. Ehsani, B. Jaleh, M. Nasrollahzadeh, *Journal of Power Sources*, 2014, **257** , 300-307.

[11] M.W. Mehrens, J. Schenk, P.M. Wilde, E. Abdelmula, P. Axmann, J. Garche, *Journal of Power Sources, 2002,* **105** , 182.

[12] C.D. Lokhande, T.P. Gujar, V.R. Shinde, Rajaram S. Mane, Sung-Hwan Han, *Electrochem. Communi*, 2007, **9**, 1805-1809.

[13] T. Takamori and L. D. David, *Am. Ceram. Soc. Bull*, 1986, **65**, 1282.

[14] Y. Hakuta, T. Haganuma, K. Sue, T. Adschiri, and K. Arai, *Mater. Res. Bull,* 2003, **38,** 1257.

[15] G. Gowda, J. *Mater. Sci. Lett,*1986, **5** , 1029.

[16] S. Ramanathan, M. B. Kakade, S. K. Roy, and K. K. Kutty, *Ceram. Int*, 2003, **29,** 477.

[17] Y. C. Wu, S. Parola, O. Morty, M. Villanutva-Ibaanez, and J. Mugnier, *Opt. Mater*, **2005, 27**, 1471.

[18] M.A. Bavio, G.G. Acosta, T. Kessler, *Journal of Power Sources*, 2014, **245**, 475-481.

[19] Q. Xu, S.-X. Gu, L. Jin, Y.-e. Zhou, Z. Yang, W. Wang, X. Hu, *Sensors and Actuators B*: Chemical, 2014, **190** , 562-569.

[20] A. Ehsani, F. Babaei, M. Nasrollahzadeh, *Applied Surface Science*, 2013, **283** , 1060-1064.

[21] A. Ehsani, M. Mahjani, M. Bordbar, S. Adeli, *Journal of Electroanalytical Chemistry*, 2013, **710** , 29-35.

[22] A. Ehsani, M. Mahjani, M. Jafarian, A. Naeemy, *Electrochimica Acta*, 2012, **71,** 128-133.

[23] A. Ehsani, M.G. Mahjani, M. Jafarian, A. Naeemy, *Progress in Organic Coatings*, 2010, **69 ,**510-516.

[24] M. Mahjani, A. Ehsani, M. Jafarian, *Synthetic Metals*, 2010, **160,** 1252-1258.

[25] Z. Ežerskis, Z. Jusys, *Journal of applied electrochemistry*, 2001, **31,** 1117-1124.

[26] A. Ehsani, S. Adeli, F. Babaei, H. Mostaanzadeh, M. Nasrollahzadeh, *Journal of Electroanalytical Chemistry*, 2014, **713**, 91-97.

[27] J. Shabani-Shayeh, A. Ehsani, MR. Ganjali, P. Norouzi, B. Jaleh, *Applied Surface Science*, 2015, **353** , 594-599.

[28] B.O. Park, C.D. Lokhande, H.S. Park, K.D. Jung, O.S. Joo, Mater. Chem. Phys, 2004, **86** 239.

[29] F. Cao, J. Prakash, *J. Power Sources,* 2001, **92** , 40.

[30] H.J. Bang, W. Lu, F. Cao, J. Prakash, *J. Electrochem. Comm. 2000,* **2** , 653.

[31] M.W. Mehrens, J. Schenk, P.M. Wilde, E. Abdelmula, P. Axmann, J. Garche, *J. Power Sources, 2002,* **105** , 182.

[32] A. Pandolfo, A. Hollenkamp, *Journal of power sources*, 2006,**157,** 11-27.

[33] G.S. Gund, D.P. Dubal, S.S. Shinde, C.D. Lokhande, *ACS applied materials & interfaces*, 2014, **6,** 3176-3188.

[34] A. Ehsani, M.G. Mahjani, R. Moshrefi, H. Mostaanzadeh, J.S. Shayeh, *RSC Advances*, 2014 ,**4** , 20031-20037.

[35] Z. Fan, J. Yan, T. Wei, L. Zhi, G. Ning, T. Li, F. Wei, *Advanced Functional Materials*, 2011, **21** , 2366-2375.